Chip-scale Optical Resonator Enabled Synthesizer

(CORES) Miniature systems for optical frequency synthesis

J. E. Bowers[1*], A. Beling[2], D. Blumenthal[1], A. Bluestone[1], S. M. Bowers[2], T. C. Briles[3], L. Chang[1], S. A. Diddams[3], G. Fish[4], H. Guo[5], T. J. Kippenberg[5], T. Komljenovic[1], E. Norberg[4], S. Papp[3], M. H. P. Pfeiffer[5], K. Srinivasan[3], L. Theogarajan[1], K. J. Vahala[6], N. Volet[1]

[1]UCSB, [2]UVA, [3]NIST, [4]Aurrion, [5]EPFL, [6]Caltech [*]bowers@ece.ucsb.edu

Invited Paper

***Abstract*—An approach for a low-power chip-scale package is described, that provides a laser output with a programmable frequency across 50 nm of bandwidth centered at 1550 nm, and a resolution of one part in 10^{14}.**

***Keywords*—Tunable lasers, narrow linewidth, optical frequency combs, second-harmonic generation, octave spanning, heterogeneous integration.**

I. Introduction

A very successful approach for the precise synthesis and control of optical frequencies at a level comparable to microwave techniques is based on femtosecond laser frequency combs. However, their role in real-world applications is limited, due to the size, weight, power and cost of existing mode-locked lasers. Another class of parametric frequency combs has later emerged based upon chip-compatible monolithic microresonators [1]. This new technology, together with rapidly maturing integrated active and passive photonic elements [2], provides the opportunity for another revolutionary advance in optical frequency synthesis. In this work, we describe a chip-scale optical resonator enabled synthesizer (CORES), shown in Fig. 1.

This approach is aimed at fully integrating active and passive components (including control electronics) of a comb-based optical frequency synthesizer on a silicon (Si) chip having dimensions on the centimeter scale. We leverage microcomb technology to realize an arbitrary optical frequency synthesizer controlled by a radio-frequency (RF) reference input.

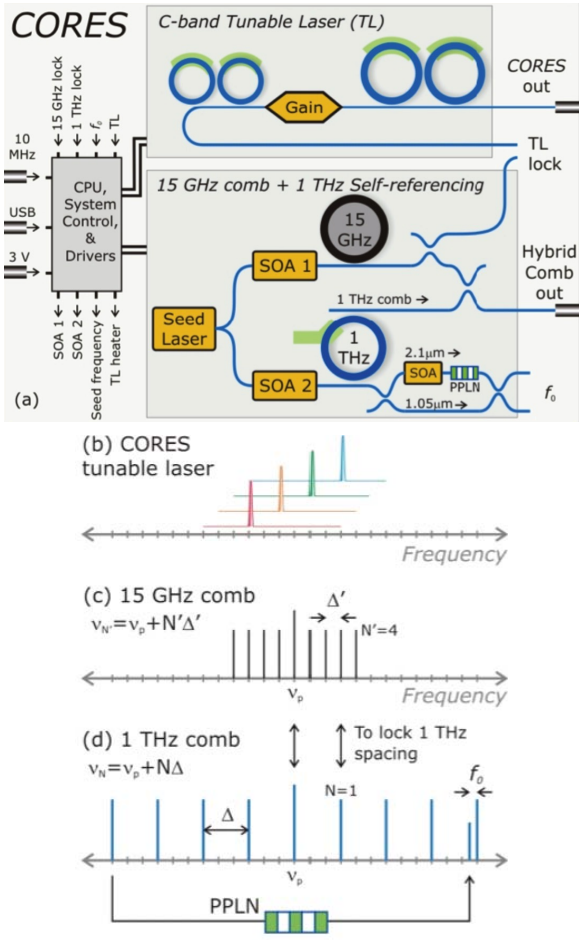

Figure 1: Schematic of the CORES architecture.

I. Widely Tunable Lasers

A narrow linewidth optical output is extremely useful for spectrally efficient high bandwidth communication. The best linewidth for a widely tunable laser (> 40 nm) on chip has been in the hundreds of kHz mainly due to the internal losses of the laser cavity [3]. By integrating III-V materials to Si and/or oxides and nitrides of Si, the III-V absorption losses can be lowered, thereby increasing the quality factor Q of the laser cavity, which results in linewidths of a few tens of kHz [4].

The CORES synthesizer output is a widely tunable laser similar to the one shown in Fig. 2. It consists of a semiconductor optical amplifier (SOA) heterogeneously integrated on a Si waveguide, and surrounded on each side by a pair of coupled ring microresonators (CRRs). The periodic reflectance spectra of these CRRs have different periods, and

This work supported by DARPA MTO DODOS contract (HR0011-15-C055).

lasing occurs at the wavelengths where the reflectance peaks are aligned (Vernier effect). In addition to providing large suppression ratios of longitudinal modes (> 40 dB) [5], this mechanism allows tuning the emission wavelength by resistive heating the CRRs. Wide tuning ranges have recently been demonstrated both in the C band [5] and in the O band (> 54 nm) [6] with a frequency setting repeatability of ±100 MHz and an output power larger than 10 mW. These high *Q*-factor CRRs also provide large reduction in linewidth (< 100 kHz) [6], which is beneficial for the CORES design.

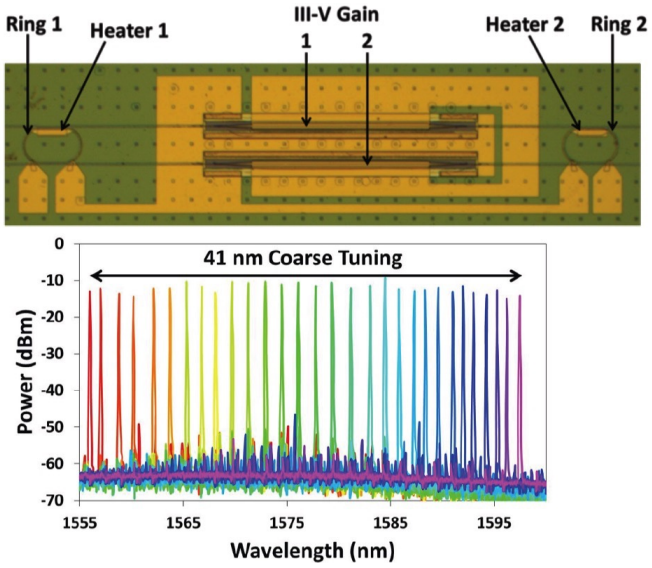

Figure 2: Top-view picture and typical tuning range of the Vernier ring tunable laser.

II. Optical Frequency Combs

The frequency synthesizer of the CORES architecture includes two other microring resonators described in the next subsections. They are pumped with a single narrow-linewidth continuous-wave (CW) seed laser operating at a frequency f_p. Second-order optical non-linearities are used to generate Kerr frequency combs with low phase noise. These ring resonators can be thermally tuned, so that f_p corresponds to the central line of their respective emitted comb spectrum. The seed laser is based on the design described in Section II.

A. Silica ring microresonator

The threshold power for parametric oscillations to occur in a ring resonator is inversely proportional to its free spectral range (FSR) and to the square of its total quality factor [7]. The silica (SiO_2) ring resonator in the CORES architecture is designed to generate a comb with a very small spacing (corresponding to the ring FSR) of 15 GHz and spanning just 50 nm around 1550 nm. To mitigate the small spacing and reduce the threshold power, a high *Q*-factor (>10^8) is required. Silica-on-silicon wedge resonators have demonstrated the required Q factors [8] as well as low-power comb generation [7]. In the present work a SiO_2 *ridge* waveguide is being developed for the resonator as illustrated in Fig. 3. This will enable the incorporation of an integrated waveguide for coupling to other components.

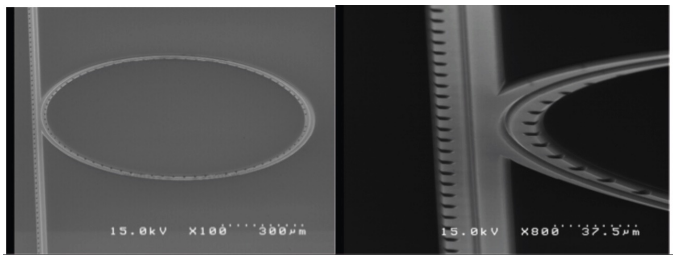

Figure 3: SEM of a SiO_2 ridge resonator with integrated waveguide coupling. The process flow is a modification of the process flow used to create high-Q wedge resonators [8].

One of the comb lines emitted from the SiO_2 ring resonator is phase-locked to the widely tunable laser described in Section II. This is achieved by controlling the optical heterodyne beat frequency between them with an electronic phase-locked loop (PLL) [9]. The beat frequency is forced to oscillate in phase with respect to a reference RF of 10 MHz provided by a direct digital synthesizer (DDS). The 15-GHz SiO_2 microcomb thus serves as a frequency reference for the tunable laser. Furthermore, the 15-GHz spacing is photo-detected and phase-locked to a second RF input. Feedback is applied to the ring to thermally tune and stabilize this spacing.

B. Silicon nitride microresonator

This ring resonator is designed to generate a 1-THz spacing comb with an octave bandwidth. This large spacing allows to have a moderate *Q*-factor (~10^6) for a relatively low threshold power. Nearly stoichiometric silicon nitride (Si_3N_4) is used for the resonator. It is fabricated with the photonic Damascene process developped at EPFL [10], which allows thick (> 800 nm) and crack-free films. As summarized in Fig. 4, Si_3N_4 is deposited onto a pre-structured substrate, planarized using chemical mechanical polishing and a dense pattern around the waveguides relaxes the Si_3N_4 film.

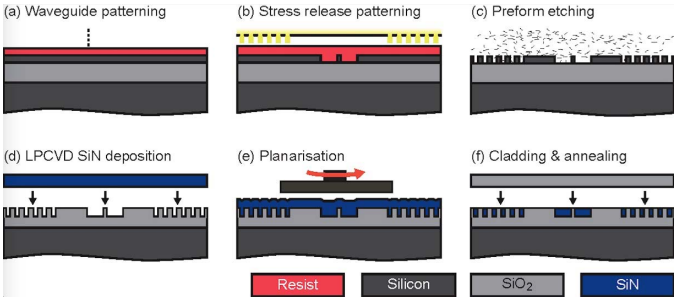

Figure 4: Schematic process flow of the photonic Damascene process for integrated Si_3N_4 waveguides.

The 1-THz mode spacing is stabilized by optical heterodyne of the 1st-order 1-THz comb line and the 67th-order

15-GHz comb line. Another on-chip PLL forces this beat frequency to oscillate in phase with respect to a third reference RF. The purpose of the 1-THz comb is to phase-coherently connect the pump seed laser frequency f_p to this known input RF.

In this work, temporal soliton formation is used to ensure that the Kerr combs span at least an octave [11]. Furthermore, a careful design of the anomalous GVD window of the resonator, allows the generatation of double dispersive waves (at the zero-dispersion points), as illustrated in Fig. 5. These typically high-intensity features in the emitted spectra are of primary importance to ensure sufficient signal-to-noise ratio (SNR) for successful stabilisation of the comb. Indeed, once the 1-THz comb spacing is stabilized, the comb output passes through a dichroic splitter to separate out comb light near 2-µm, which is then amplified by a semiconductor optical amplifiers (SOA) [12] and frequency doubled through an integrated periodically-poled lithium niobate (PPLN) waveguide [13].

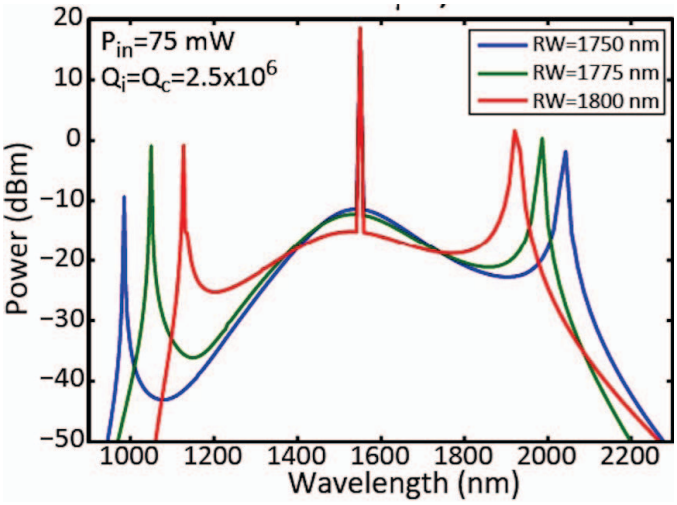

Figure 5: Simulation of double-dispersive waves generated in a ring micro-resonator with different ring widths (RW).

The doubled 2-µm light and filtered 1-µm comb light are then combined with a 2x2 directional coupler and balanced detected with a high common-mode rejection ratio (CMRR). A transimpedance amplifier (TIA) is then used to ensure optimum conversion gain, noise, and bandwidth performance. This *f*-2*f* interferometry then yields the carrier-offset frequency signal with suppression of the relative intensity noise (RIN), from which the absolute value of the frequency f_p is deduced with respect to the RF clock. Dispersion engineering of the 1-THz Si_3N_4 ring is critical for the generation of sufficient comb bandwidth, sufficient comb line power near 2 µm for second-harmonic generation and for realizing frequency alignment of the resonator such that the carrier-offset frequency is an electronically measurable signal smaller than 10 GHz.

III. Semiconductor Optical Amplifiers

SOAs are critical components for many kinds of photonic integrated circuits to increase output power or maintain signal levels as the signal propagates throughout a large number of optical components [15]. This is particularly true for the CORES architecture where 2 relatively weak frequency lines are at the center of the comb stabilization procedure.

In this work, SOAs are integrated on a heterogeneous silicon/III-V photonics platform. In particular, 2-µm SOAs are developped with a broad-area composed of InGaAs quantum wells bonded onto a Si waveguide. The hybrid optical mode is laterally confined by the Si waveguide, while a portion of the mode overlaps the III–V active region [16]. The III–V mesa is terminated on both sides by a lateral tapering of the III–V material, causing the hybrid active mode to couple into a passive Si waveguide mode. A Fabry–Perot cavity is then formed by the polished Si facets.

IV. Second-Harmonic Generation

As mentioned in Section III, *f*-2*f* comb stabilization relies on the frequency doubling of light emitted near 2 µm. In this work, second-harmonic generation (SHG) is based on an integrated PPLN device composed of a Si_3N_4 waveguide, as schematized in Fig. 6. Surface poling of thin film lithium niobate has been recently developed [13]. This technology represents a breakthrough for on-chip non-linear optics as the propagation loss is ultra low and the conversion efficiency can be orders of magnitude higher than previous state-of-the-art.

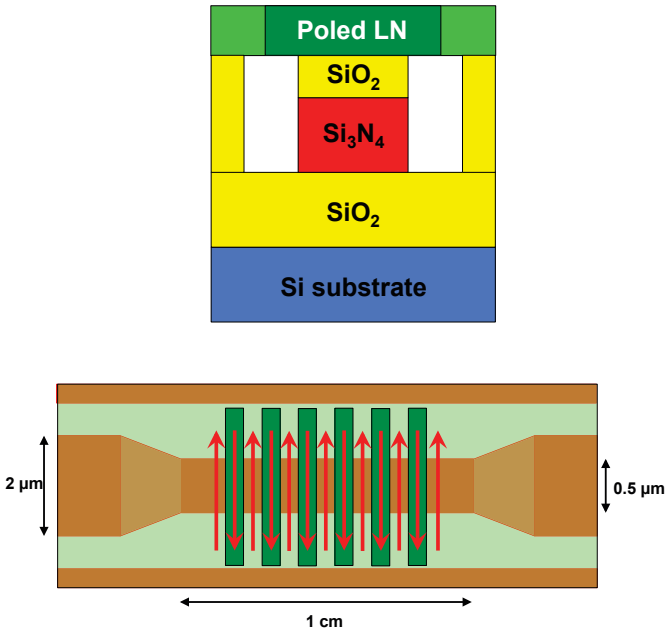

Figure 6: Cross-section and top-view schematic of a PPLN thin film integrated on Si_3N_4. The red arrows indicate the orientation of the electric polarization [13].

V. Electronics

The electronic chips used to drive and control all of the photonic elements in the synthesizer are fabricated with a 65-nm CMOS process. The various control loops can be divided

into four main parts: 1) the 1-THz comb offset frequency measurement, 2) the control and stabilization of the tunable laser, 3) locking the 15-GHz comb to the 10-MHz reference via clock multiplication through a DDS, and 4) locking the 1-THz comb to the 15-GHz comb.

One of the key challenges in the CORES architecture is to detect the offset frequency of the 1-THz comb, via the *f*-2*f* technique mentioned in Section III. The power of the beat note out of the PPLN is <100 nW, and the beat frequency of the PPLN output with the nearest comb line of the 1 THz comb is of the order of 15 GHz. Therefore, the signal cannot be used directly to lock the microcomb. The photodiode signal is then first amplified using a low-noise transimpedance amplifier (TIA) with at least 30-40 dB of gain. Since the SNR is quite low, the signal needs to be adequately bandlimited for noise performance. The center frequency of the bandpass is tuned by using a PLL loop with a VCO based on the bandpass filter. Since the offset frequency is unknown initially, a search timer will set the VCO to the highest oscillation frequency and then wait during a prescribed period. If lock detect is not asserted, then the divider is incremented and the procedure repeated until a lock is attained. Once lock is achieved, the PLL loop is frozen in this state.

VI. PHOTODIODES

The critical parameters for the performance of a photodiode (PDs) operated under pulsed operation are its non-linearities and its saturation. The non-linearities degrade the spectral purity of the signal. They are characterized by the AM–PM coefficient, which describes the coupling between the amplitude noise on the optical intensity and the phase noise on the microwave signal. When a high density of photo-generated carriers is present in the diode, a screening of the applied bias is created. This space charge effect slows down the diode response time and induces AM-PM.

Uni-traveling carrier (UTC) photodiodes incorporate an undepleted *P*-layer for the light absorber and electrons are injected into a non-absorbing drift region. Since there are only electrons in the depletion region, the space-charge effect is greatly suppressed, because electrons have higher velocity compared to holes. This allows for the UTC-PDs to reach higher bandwidth as compared to conventional *PIN*-PDs. Modified uni-traveling carrier (MUTC) photodiodes further reduce the space charge effect by incorporating a "cliff" layer to control the relative electric field strength in the absorber and collector regions [14]. MUTC-PDs thus effectively suppress the space charge effect, in addition to exhibit high linearity, which limits the impact of laser RIN on the stability of the signal. Thermal management is also a key issue for the design of PDs delivering high power.

To facilitate efficient low-noise photo-detection, MUTC waveguide PDs on SOI are thus used, with near-to-unity quantum efficiency, as illustrated in Fig. 7. The improved electric field control of these devices make them ideal candidates for high-efficiency high-power PDs at low bias voltage [14]. Surface-normal illuminated MUTC-PDs achieving record-high RF output power level, high linearity and very low amplitude-to-phase noise conversion have been recently developed. To integrate the MUTC structure as a waveguide PD on the Si/SiN platform, an inverse Si taper is used as optical coupling scheme [17]. In this approach, the width of the light-feeding Si wire waveguide determines the coupling into the absorber, which results in superior control of the absorption profile. Optimum high power capability, improved linearity, and a low AM-PM coefficient become feasible thanks to the optimized absorption profile from the engineering of the confinement factor.

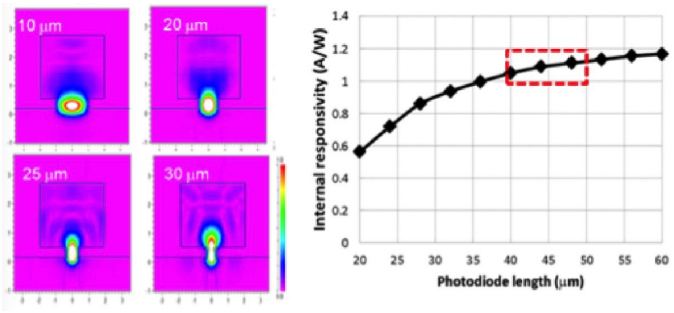

Figure 7: Intensity in waveguide MUTC PD with inverse taper [14]. Light from an underlying Si_3N_4 waveguide (not shown here) can be coupled into the Si wire using tapered waveguide couplers as described in [17]. b) Simulated responsivity.

VII. HETEROGENEOUS INTEGRATION PLATFORM

The CORES platform is fabricated using heterogeneous integration on a Si substrate [11]. It includes passive waveguide types (Si wire, Si rib, SiN) to facilitate different routing densities, mode profiles, and thermo-optic behaviors, and active component process modules for laser, optical amplifier, and photodetector functions. Evanescent mode converters provide a low-loss conduit between Si and InP layers to optimally place the optical mode within the device structures. Heterogeneous integration of III-V materials is accomplished by locally placing and bonding "chiplets" of custom tailored, unprocessed InP epitaxial material onto the silicon wafer [11]. Subsequent lithography and etch steps are used to form the active devices. Further deposition and etch processing steps finally encapsulate the InP device structures with dielectric materials and form metal interconnects and contacts for interfacing with driver and control circuitry.

VIII. CONCLUSIONS

The CORES system utilizes a heterogeneous photonic/electronic approach to implement direct digital synthesis of optical frequencies in a single integrated chip-scale package. It combines the best materials and technologies for each element of the synthesizer, *i.e.*, 1) Low-noise pump lasers integrated with low-loss integrated photonics, 2) 1-THz Si_3N_4 ring comb generator for power-efficient microwave-to-optical connection and 15-GHz SiO_2 comb generator to form an absolute frequency grid, 3) Narrow linewidth CW laser output digitally tuned at Hertz level around 1550 nm, and 4) Si

photonics and CMOS electronics for a high-performance and fully integrated compact package at low cost.

The CORES system should enable unprecedented frequency precision that can be deployed on smaller mobile platforms for a wide variety of military and sensing purposes. It will also impact commercial applications, including coherent, high-bandwidth optical communications, medical and environmental diagnostics, and advanced electronic/optical instrumentation.

ACKNOWLEDGMENT

The authors would like to thank Robert Lutwak, Rob Ilic, Qing Li, Nate Newbury, Laura Sinclair, Jordan Stone, Ye Wang, Daron Westly, Xiaojun Xie and Michael Zervas for helpful discussions.

REFERENCES

[1] P. Del Haye, A. Schliesser, O. Arcizet, T. Wilken, R. Holzwarth and T. J. Kippenberg, "Optical frequency comb generation from a monolithic microresonator", Nature **450**, 1214 (2007).

[2] M. J. R. Heck, J. F. Bauters, M. L. Davenport, J. K. Doylend, S. Jain, G. Kurczveil, S. Srinivasan, Y. Tang and J. E. Bowers. "Hybrid Silicon Photonic Integrated Circuit Technology", IEEE J. Sel. Topics Quant. Electron. **19**, 6100117 (2013).

[3] J. C. Hulme, J. K. Doylend, and J. E. Bowers, "Widely tunable Vernier ring laser on hybrid silicon", Opt. Express **21**, 19718-19722 (2013).

[4] T. Komljenovic, *et al*., "Heterogeneous Silicon Photonic Integrated Circuits", J. Lightwave Technol. **34**, 20-35 (2016).

[5] S. Srinivasan, M. Davenport, T. Komljenovic, J. Hulme, D. T. Spencer, and J. E. Bowers, "Coupled-Ring-Resonator-Mirror-Based Heterogeneous III–V Silicon Tunable Laser", IEEE Photon. J. **7**, 2700908 (2015).

[6] T. Komljenovic, S. Srinivasan, E. Norberg, M. Davenport, G. Fish, and J. E. Bowers, "Widely Tunable Narrow-Linewidth Monolithically Integrated External-Cavity Semiconductor Lasers", IEEE J. Sel. Topics Quantum Electron. **6**, 1501909 (2015).

[7] J. Li, H. Lee, T. Chen, and K. J. Vahala, "Low-Pump-Power, Low-Phase-Noise, and Microwave to Millimeter-Wave Repetition Rate Operation in Microcombs", Phys. Rev. Lett. **209**, 233901 (2012).

[8] H. Lee, T. Chen, J. Li, K. Y. Yang, S. Jeon, O. Painter and K. J. Vahala, "Chemically etched ultrahigh-Q wedge-resonator on a silicon chip," Nature Photon. **6**, 369–373 (2012).

[9] Th. Udem, J. Reichert, R. Holzwarth, and T. W. Hänsch, "Absolute Optical Frequency Measurement of the Cesium D1 Line with a Mode-Locked Laser", Phys. Rev. Lett. **82**, 3568 (1999).

[10] M. H. P. Pfeiffer, A. Kordts, V. Brasch, M. Zervas, M. Geiselmann, J. D. Jost, and Tobias J. Kippenberg, "Photonic Damascene process for integrated high-Q microresonator based nonlinear photonics", Optica **3**, 20 (2016).

[11] Q. Li, T. C. Briles, D. A. Westly, J. R. Stone, B. R. Ilic, S. A. Diddams, S. B. Papp, and K. Srinivasan, "Octave-spanning microcavity Kerr frequency combs with harmonic dispersive-wave emission on a silicon chip", Frontiers in Optics/Laser Science, Paper FW6C.5 (2015).

[12] N. Volet, A. Spott, E. J. Stanton, M. L. Davenport, J. Peters, J. Meyer, and J. E. Bowers, "Semiconductor optical amplifiers at 2.0-μm wavelength heterogeneously integrated on silicon", in Conference on Lasers and Electro-Optics (2016).

[13] L. Chang, Y. Li, N. Volet, L. Wang, J. Peters, and J. E. Bowers, Optica, in press.

[14] Z. Li, Y. Fu, M. Piels, H. Pan, A. Beling, J. E. Bowers, and J. C. Campbell, "High-power high-linearity flip-chip bonded modified uni-traveling carrier photodiode", Opt. Express **19**, B385–B390 (2011).

[15] M. L. Davenport, S. Skendžić, N. Volet, J. C. Hulme, M. J. R. Heck, and J. E. Bowers, "Heterogeneous Silicon/III-V Semiconductor Optical Amplifiers", IEEE J. Sel. Topics Quantum Electron., in press.

[16] A. Spott, M. Davenport, J. Peters, J. Bovington, M. J. R. Heck, E. J. Stanton, I. Vurgaftman, J. Meyer, and J. Bowers, "Heterogeneously integrated 2.0 μm CW hybrid silicon lasers at room temperature", Opt. Lett. **40**, 1480-1483 (2015).

[17] M. Piels, J. F. Bauters, M. L. Davenport, M. J. R. Heck, and J. E. Bowers, "Low-Loss Silicon Nitride AWG Demultiplexer Heterogeneously Integrated With Hybrid III–V/Silicon Photodetectors", J. Lightwave Technol. **32**, 817-823 (2014).